# Field dependence of the electronic phase separation in $Pr_{0.67}Ca_{0.33}MnO_3$ by small angle magnetic neutron scattering

Silvana Mercone, Vincent Hardy, Christine Martin, Charles Simon,
*Laboratoire CRISMAT, UMR 6508 du CNRS et de l'Institut Supérieur de la Matière et du Rayonnement, 14050 CAEN, France.*

Damien Saurel, Annie Brûlet,
*Laboratoire Léon Brillouin, CE SACLAY, 91191 Gif/Yvette, France*
(March 22, 2022)

arXiv:cond-mat/0308534v1 26 Aug 2003

We have studied by small angle neutron scattering the evolution induced by the application of magnetic field of the coexistence of ferromagnetism (F) and antiferromagnetism (AF) in a crystal of $Pr_{0.67}Ca_{0.33}MnO_3$. The results are compared to magnetic measurements which provide the evolution of the ferromagnetic fraction. These results show that the growth of the ferromagnetic phase corresponds to an increase of the thickness of the ferromagnetic "cabbage" sheets.

PACS numbers: 64.75 g,71.12 Ex, 75.25+z

## I. INTRODUCTION

It was recently proposed that the ground state of manganites which displays colossal magnetoresistive (CMR) properties [1] could be an electronic phase separation [2,3]. This is a very elegant manner to interpret the CMR properties by percolation of a metallic ferromagnetic phase in an insulating antiferromagnetic matrix. A small change of the fraction or of the arrangement of the domains can induce percolation. In order to go further in the percolation models, it is very important to determine the size and the shape of the domains. Small angle neutron scattering (SANS) is indeed a very powerful technique to study the phase separation between a ferromagnet and an antiferromagnet since the contrast between them is very large (the AF does not scatter at small angle) [5,6,4]. Among the manganites, the $Pr_{1-x}Ca_xMnO_3$ series is one of prime interest, because Pr and Ca are about the same size and hence minimize the cationic size mismatch effect. $Pr_{1-x}Ca_xMnO_3$ magnetic phase diagram presents different states depending on the x value. For the higher $Mn^{3+}$ contents (typically x=0.2), the compounds are ferromagnetic at low temperature, and for larger x values (typically x=0.4) they are orbital ordered, antiferromagnetic CE like type. In between, the composition x=0.33, studied here, shows a mixing of F and AF phases as shown by neutron diffraction [7]. For these compositions close to x=0.33, existence of the phase separation is now well proved by magnetoresistance, magnetization and specific heat studies [8,9]. Small angle neutron scattering has shown that at low temperature (below 30K), the structure is that of a "cabbage" with 2D sheets (stripes) of about 2.5nm of thickness [4]. In the present paper, we propose to study the influence of the application of a magnetic field on this phase separation during percolation of the metallic phase.

## II. EXPERIMENTAL

Using the floating-zone method with feeding rods of nominal compositions $Pr_{0.7}Ca_{0.3}MnO_3$, several-cm-long single crystals were grown in a mirror furnace. Samples were cut out of the central part of these crystals and were analyzed by EDS: their cationic compositions are homogeneous and were found to be x= 0.33. Magnetization and transport measurements were performed to check their quality. The samples were then powdered in order to perform neutron diffraction. The powder diffraction patterns were recorded in the G41 spectrometer in Orphée reactor from 1.5K to 300K. It presents at 1.5K both a F component and an AF one. Tc is about 100K and $T_N$ about 115K. The structures were refined using the Fullprof program, in the Pbnm symmetry ($a_p\sqrt{2}$, $a_p\sqrt{2}$, $2a_p$). The previous small angle neutron scattering study [4] was performed on the same powdered sample. In the present experiment, we have studied a part of the same sample but in the form of a single crystal which was cut out of the rod without any specific orientation.

Small angle neutron scattering were performed on PAXY spectrometer at the Orphée reactor. Three different experimental configurations were used: the first is with a wavelength of 10 Å and a sample-multidetector distance of 5.6 m, allowing to study Q values between 4 $10^{-3}$ and 4 $10^{-2}$ $Å^{-1}$ . The second one is with a wavelength of 4.5 Å and a sample detector distance of 5.6 m, allowing to reach higher values between $10^{-2}$ and $10^{-1}$ $Å^{-1}$. The third one is with a wavelength of 4.5 Å and a sample detector distance of 1.5 m, allowing to reach higher values up to 4 $10^{-1}$ $Å^{-1}$. The sample was introduced in a cryostat with a superconducting split coil and aluminum windows. The magnetic field is applied in an horizontal plane, perpendicular to the neutron beam. Different orientations of the crystal were studied and we have found that the scattering is roughly isotropic in this range of wave vectors. Few parasitic reflections were re-

moved before data treatment. In order to subtract the background signal, an empty cell was measured. The calibration of the spectrometer was performed with a Plexiglas sample following the procedure given in reference [10]. After subtraction of the background, normalization by the Plexiglas sample, the scattering function is presented in absolute units ($cm^{-1}$). We have systematically neglected the inelastic spin wave corrections.

## III. RESULTS

### A. Magnetization versus magnetic field at 30K

We have measured the magnetization of the sample as function of the magnetic field in a Quantum Design PPMS magnetometer up to 5.9T (fig. 1). The temperature of 30K was chosen because the ferromagnetic fraction of the sample reaches 100% at 5.9T. Let us describe this magnetic hysteresis curve. Between 0 and 1T, the spins of the ferromagnetic part of the sample are gradually oriented parallel to the applied field. Between 1 and 3T, the sample is partly ferromagnet and partly antiferromagnet. The slope observed in this range is mainly due to the susceptibility of the antiferromagnetic part. Between 3 and 5.9T, the system transforms itself smoothly to pure ferromagnetic system. When the magnetic field is removed, the system remains ferromagnetic. Below 1T, ferromagnetic domains appear, leading to a zero magnetization in zero field. From the fit of this curve, we have extracted two important parameters, the ferromagnetic fraction $\phi$ and the susceptibility of the antiferromagnetic part $\chi_{antif}$ as functions of the applied field B. Let us now describe the results of small angle neutron scattering under the same experimental procedure.

### B. Orientation of the spins along the magnetic field

As reported in the previous study [4], the scattered intensity I(Q) decreases in $Q^{-2}$ over a wide range of wave vectors Q, characteristic of the behavior of a powder of 2D sheets without any correlations among them [11]. In this range of Q (0.02 to 0.1 $Å^{-1}$), the small angle scattering pattern at 30K in zero field (fig. 2 a) is isotropic. This is due to the fact that the ferromagnetic domains and the domains of the phase separation are both isotropic. The application of a magnetic field larger than 2T ( fig. 2b at 2T) provides anisotropic iso-intensity curves which can be fitted by parts of circles. This anisotropy is specific of the effect of the orientation of the spins along the applied magnetic field. The intensity $I(Q,\alpha)$ is proportional to $I(Q)\ \sin^2\alpha$ where Q is the modulus of the scattering vector and $\alpha$ the angle between the vector Q and the vector M (parallel to B) [10]. In this range of Q, in which the Q dependence is in $Q^{-2}$ (the "cabbage structure"), the lines of iso-intensity correspond to $Q=Q_0 \sin\alpha$, which are two parts of circles. This is exactly what is observed here (as shown on fig 2b). This very pecular behavior is thus explained. Consequently, one can say that the application of a 2T magnetic field indeed corresponds to an orientation of the spins along the magnetic field. There is no transformation of the phase separation in this range of magnetic field, compatible with what was assumed in the interpretation of the magnetization curve.

### C. Magnetic field induced evolution of the phase separation

In order to analyze the Q dependence of the scattering function, we have integrated the intensity over a $\mp 15$ degrees cone for each value of Q. In addition, we have assumed from the magnetization data that the compound is completely ferromagnetic at 5.9T, so we have used the spectrum obtained under 5.9T as a background for all the other results. The application of a magnetic field, though it modifies strongly the orientation of the spins (fig. 2), does not modify too strongly the shape of the curve (fig. 3a). We have studied the magnetic field dependence of the scattering function in the medium range of Q, where the $Q^{-2}$ dependence dominates. In this range of Q, application of magnetic field decreases the scattered intensity. One can notice that the curve at 2T is slightly different from the others (the slope at small Q is smaller). We have no simple interpretation to this feature.

The same procedure was applied for the three different scattering configurations that we used. One can note that the overlap between these three configurations is very good. The results are shown on figure 3b. In absence of magnetic field, the signal is very similar to that previously published in the powdered sample, confirming that the scattering is mainly isotropic. There is a nice $Q^{-2}$ dependence sample over a large range of wave vectors. At small Q, the small angle scattering was dominated in the powder by the granular structure: it obeys to the classical Porod law [11] and varies in $Q^{-4}$. In the crystal, this contribution is much smaller than in the powdered sample (as it should be) but the $Q^{-2}$ component remains the same. On this extended range of wavevectors, it is clear that the slope at 4T is slightly different from that obtained in zero field, suggesting that the shape of the domains is also slightly different. This is not analyzed in the present work, but is related to a finite size of the in-plane ferromagnetic domains (assumed to be infinite in the "cabbage" model), inducing a fractal dimension of the objects.

In a third part of the measurement, we have decreased the magnetic field and found a signal which is completely different from the signal before and during the application of the magnetic field (fig. 3c). At 2T, the signal remains very small, indicating that the system remains

mainly ferromagnetic. At B=0, the $Q^{-2}$ component remains not visible, indicating that the signal is not originating from "cabbage" phase separation but to classical ferromagnetic quasi- isotropic Weiss domains (fig. 1).

The situation is summarized on fig. 1: Before the application of the magnetic field, the phase separation presents the "cabbage structure" with a stacking of domains ferro and antiferromagnetic. The ferromagnetic part presents classical Weiss domains. Note that the model assumes that the domains of the phase separation are infinite in two directions, but this is only an approximation and it exits in the sample parts with all the possible orientations of the sheets. Between 0 and 1T, the Weiss domains disappear. Above 3T, the antiferromagnetic part is gradually transformed into ferromagnetism. When the magnetic field is decreased, the system remains ferromagnetic, but the Weiss domains nucleate back.

### D. Analysis of the absolute values: comparison to magnetization measurements

As discussed in a previous paper [4], the $Q^{-2}$ dependence is that of uncorrelated infinite 2D sheets [11]. From this point of view, the "red cabbage" structure can be slightly misleading. In the present case, it corresponds to 2D ferromagnetic sheets in antiferromagnetic matrix which plays the role of the vacuum. If one assumes that magnetic measurements allow a precise determination of the ferromagnetic fraction $\phi$, the only adjustable parameter in this model is the thickness of the 2D sheets "t" (total thickness of the ferro and antiferromagnetic layers). Then, the thickness of the ferromagnetic sheets is $\phi$t and that of the antiferromagnetic one is (1-$\phi$)t. For such a 2D object, the scattering function is

$I_m(Q) = 2\pi\ \phi(1-\phi) t_{eff}\ \Delta\rho_m^2(B)\ Q^{-2} \frac{(1-\cos Qt)}{(Qt)^2}\ \sin^2\alpha$

which is reduced in the case of a wide dispersion of "t" values to:

$I_m(Q) = \pi\phi(1-\phi)\ t_{eff}\ \Delta\rho_m^2(B)\ Q^{-2}\ \sin^2\alpha$

where $t_{eff}$ is given by $t_{eff} = t\phi(1-\phi)$ and $\Delta\rho_m(B)$ is the magnetic contrast which depends on B since the antiferromagnetic scattering length is proportional to the applied field B. $\Delta\rho_m$ is proportional to the difference of magnetizations between ferro and antiferromagnetic phases: $\Delta\rho_m = x(M_{ferro} - M_{antif})$. The amplitude of $M_{ferro}$ in this formula will be assumed here to be constant 3.8 $\mu_B$ (its variation when the magnetic field is applied is negligible) and $M_{antif} = \chi_{antif}$ B is determined from magnetic measurements. The proportional constant $x$ is 0.27 $10^{-12}$ cm/$\mu_B$ divided by the unit volume of a formula unit 0.57 $10^{-22}$ cm$^3$, so $\Delta\rho_m^2$ =0.4 $10^{21}$ cm$^{-4}$ (1-$M_{antif}/M_{ferro}$)$^2$. Figure 4 presents $\phi$ and $\Delta\rho_m(B)^2$ values extracted from fig. 1.

Experimentally, $IQ^2$=0.3 $10^{14}$ cm$^{-3}$in zero field. This drives, using

$I_m(Q) = \pi\phi(1-\phi)\ t_{eff}\ \Delta\rho_m^2(B)\ Q^{-2}\ \sin^2\alpha$

to a parameter value $\phi$t, which is about 15 Å.

From these data, coupled to the $\phi$ and $\Delta\rho_m(B)$ values extracted from fig. 1, it is possible to extract the parameter "t" and the two parameters $\phi$t and (1-$\phi$)t, which are the thicknesses of ferromagnetic and antiferromagnetic sheets respectively as functions of magnetic field. They are shown on figure 5. On this figure, one can see that the thickness of the ferromagnetic sheets increases versus magnetic field and that the antiferromagnetic ones decreases, suggesting that only part of the thickness of the antiferromagnetic sheets switches to ferromagnetic as one increases the applied field. The simple picture in which the whole thickness of the antiferromagnetic domain switches at once does not apply here.

Recently, it was proposed [13] that the "simple" percolation model cannot apply in the same compound since the ferromagnetic order appears as long range order (larger than a few hundreds angtroms) in neutron diffraction. However, this argument does not hold in the case of cabbage structure as previously explained [4]. On the contrary, the present results demonstrate that such a percolation model is really adequate.

## IV. CONCLUSION

In conclusion, the use of the magnetic SANS technique under magnetic field, coupled to classical magnetization measurements allows to determine the magnetic field dependence of the thickness of the different magnetic domains in the phase separated $Pr_{1-x}Ca_xMnO_3$ with x=0.33 system. One can see that this transformation corresponds to a gradual irreversible switching from antiferromagnetic sheets to ferromagnetic ones, transforming the system to complete ferromagnetic state at 6T. At about 3T, the system reaches the percolation of the metallic ferromagnetic phase. This is at the origin of the colossal magnetoresistance.

## V. ACKNOWLEDGMENTS:

We acknowledge L. Hervé for sample preparation, and very important support from F. Ott and his cryostat. S. Mercone has been supported by a Marie Curie fellowship of the European community program under contract number HPMT2000-141. D. Saurel has been supported by the "région basse Normandie".

## VI. FIGURE CAPTIONS

Figure 1: The magnetization of the sample at 30K as function of magnetic field (the field is ramped up to 5.9T and down to zero). Insets: schematic drawings of the corresponding structures: before the application of the

field, the system is a coexistence at a nanoscopic scale of ferro (grey) and antiferromagnetic (white) sheets. These sheets are supposed to be infinite in the model, but different orientations of the sheets with respect to the magnetic field (applied vertically in the pictures) are present in the sample ("cabbage" structure). The application of the magnetic field first orientate the Weiss domains (up to 1T), then transforms the antiferromagnetic phase into ferromagnetism (above 3T). At 5.9T, the system is fully transformed. When the field is decreased, the system creates back Weiss domains below 1T.

Figure 2: The scattering plane at 30K without and with a magnetic field of 2T. The magnetic field is applied horizontally in fig. b.

Figure 3 a: The magnetic small angle scattering function at 30K ramping up from zero field to 5.9T for the intermediate range of wave vectors. The signal obtained at 5.9T is used as background.

Figure 3 b: The small angle scattering function at 30K at 0T and 4T ramping up from zero field. The three different experimental Q ranges are evidenced by a small gap in the curves. On these curves, the background was also chosen to be the sample itself at 5.9T where the whole sample is ferromagnetic.

Figure 3 c: The small angle scattering function at 30K at 2T and zero field after application of 6T, compared to the same curve before application of field.

Figure 4 : $\phi$ and $\Delta\rho_m(B)^2$ values extracted from fig. 1.

Figure 5 : The magnetic field dependence at 30K of the two parameters $t_F = \phi t$ and $t_{AF} = (1\text{-}\phi)t$, which are the thicknesses of the ferromagnetic sheets and the antiferromagnetic sheets respectively.


[1] For a review, see for example J.M.D. Coey, M. Viret and S. von Molnar, Adv. Phys. 48, 167 (1999) ,*Colossal Magnetoresistance, Charge Ordering and Related Properties of Manganese Oxides,* edited by C. N. R. Rao and B. Raveau (World Scientific, Singapore, 1998) and *Colossal Magnetoresistive Oxides*, edited by Y. Tokura (Gordon and Breach Science, New York, 1998).

[2] A. Moreo, S. Yunoki, E. Dagotto, Science 283, 2034 (1999)

[3] D. Khomskii, Physica B 280, 325 (2000)

[4] Ch. Simon, et al., Phys. Rev. Lett. 89, 207202 (2002)

[5] J. de Teresa et al., Nature 386, 256 (1997)

[6] P. G. Radaelli et al., Phys. Rev. B63, 172419 (2001)

[7] Z. Jirak et al., J. Magn. Magn. Mater. 53, 153 (1985)

[8] V. Hardy, A. Wahl, C. Martin, Phys. Rev. B 64, 64402 (2001)

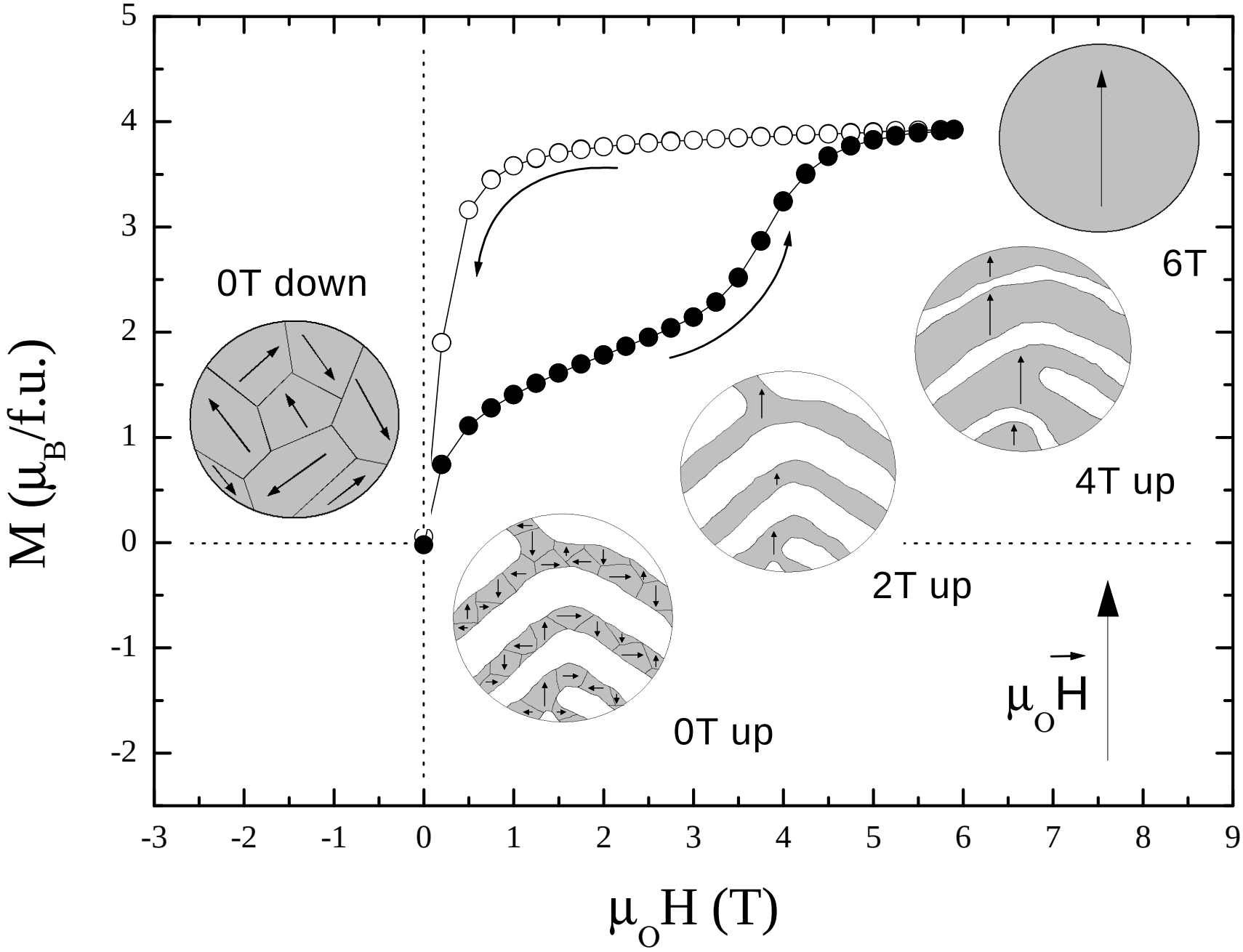
[9] I. G. Deac, J. F. Mitchell, P. Schiffer, Phys. Rev. B 63, 172408 (2001)

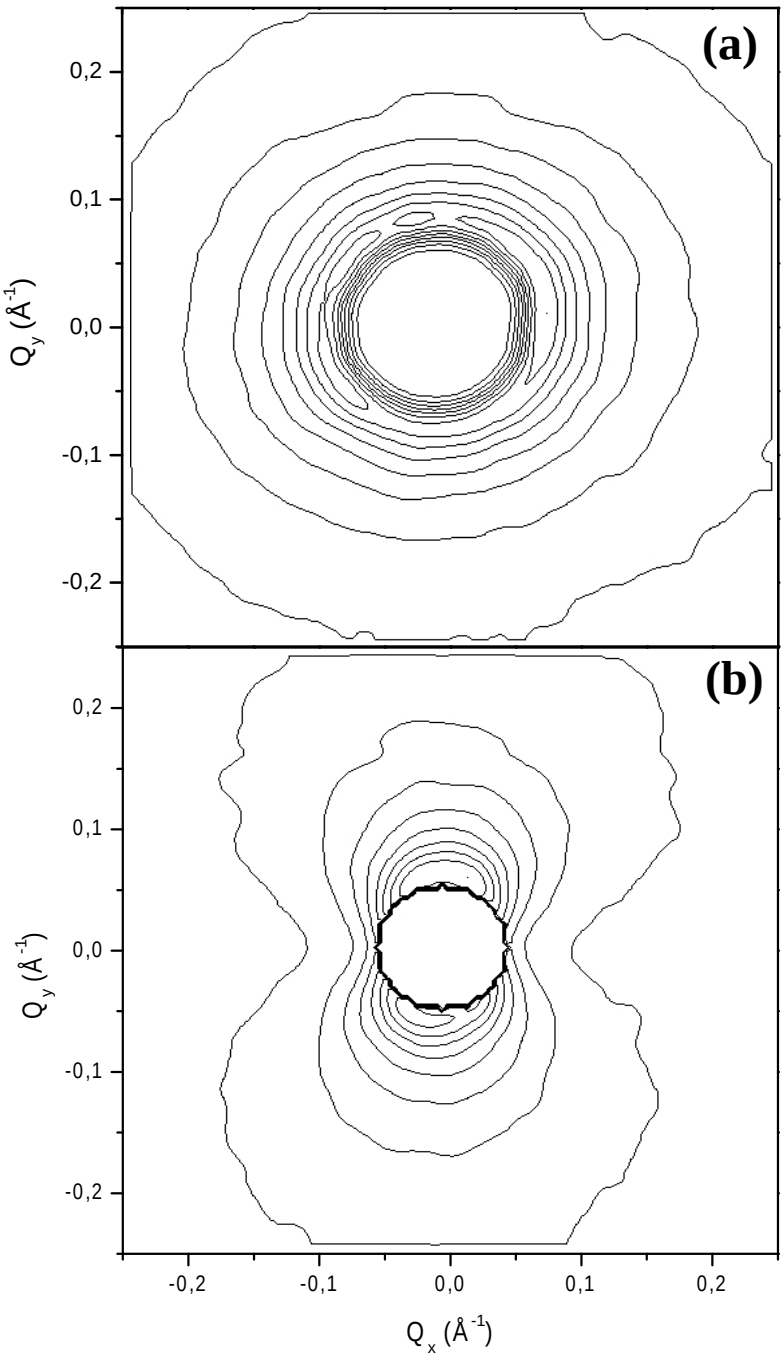
[10] "Diffusion de neutrons aux petits angles" ed. by J. P. Cotton and F. Nallet, J. de Phys. Paris IV, 9 (1999).

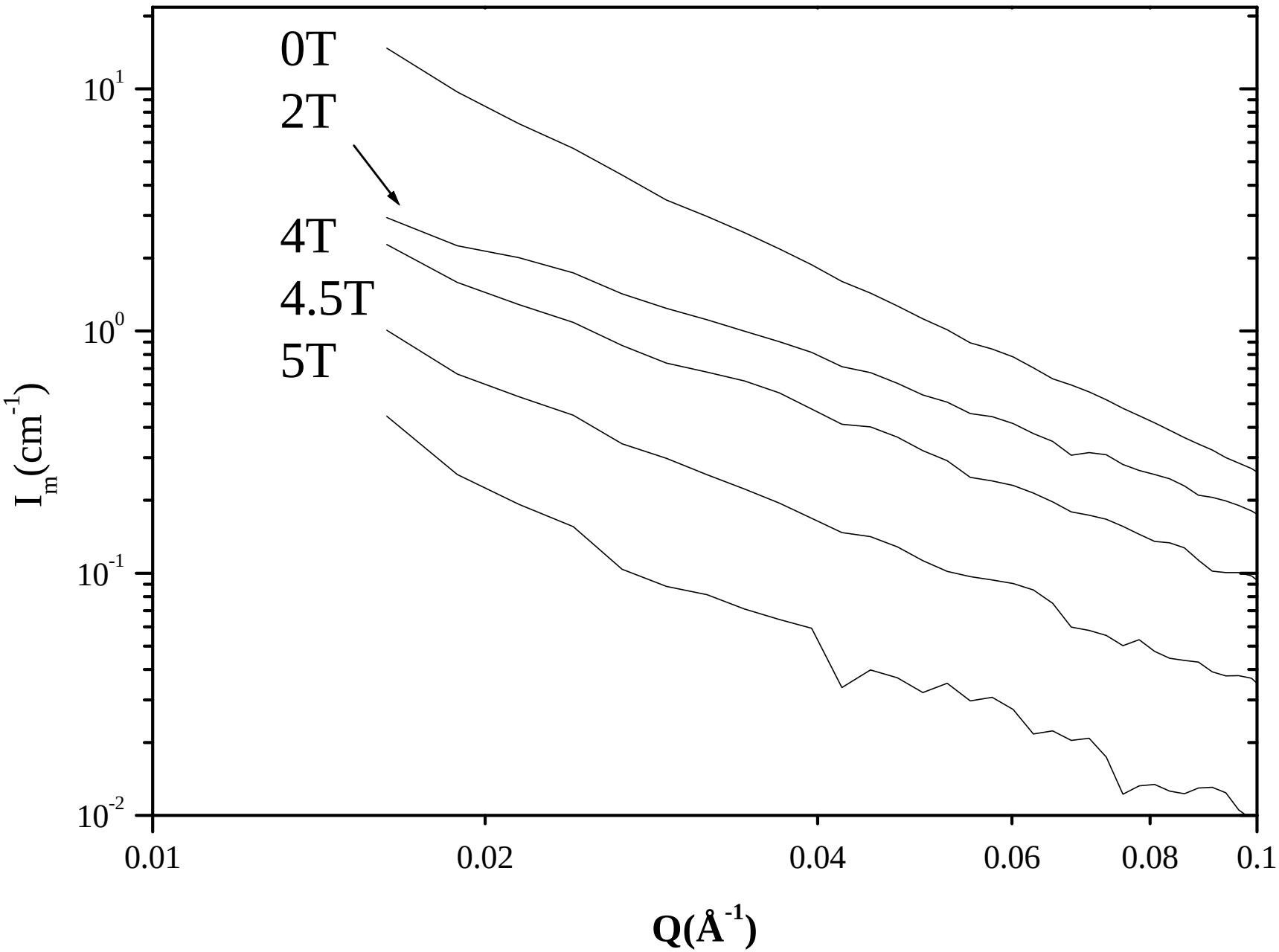
[11] G. Porod in Small Angle X-ray Scattering p.35, O. Glatter and O.Kratky Eds., Academic Press London, 1983.

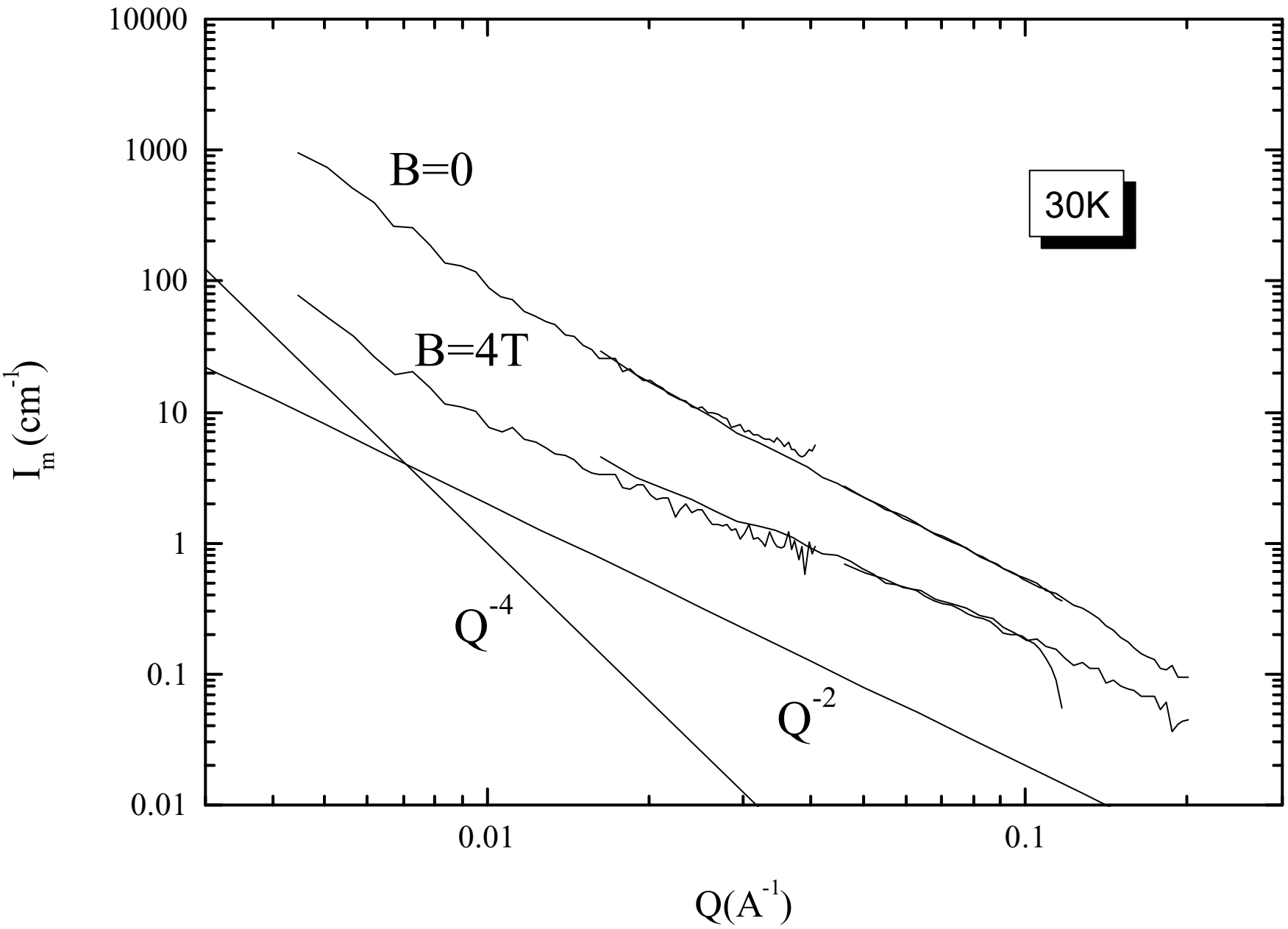
[12] F. Nallet, R. Laversanne , D. Roux, J. Phys. II 3, 487 (1993).

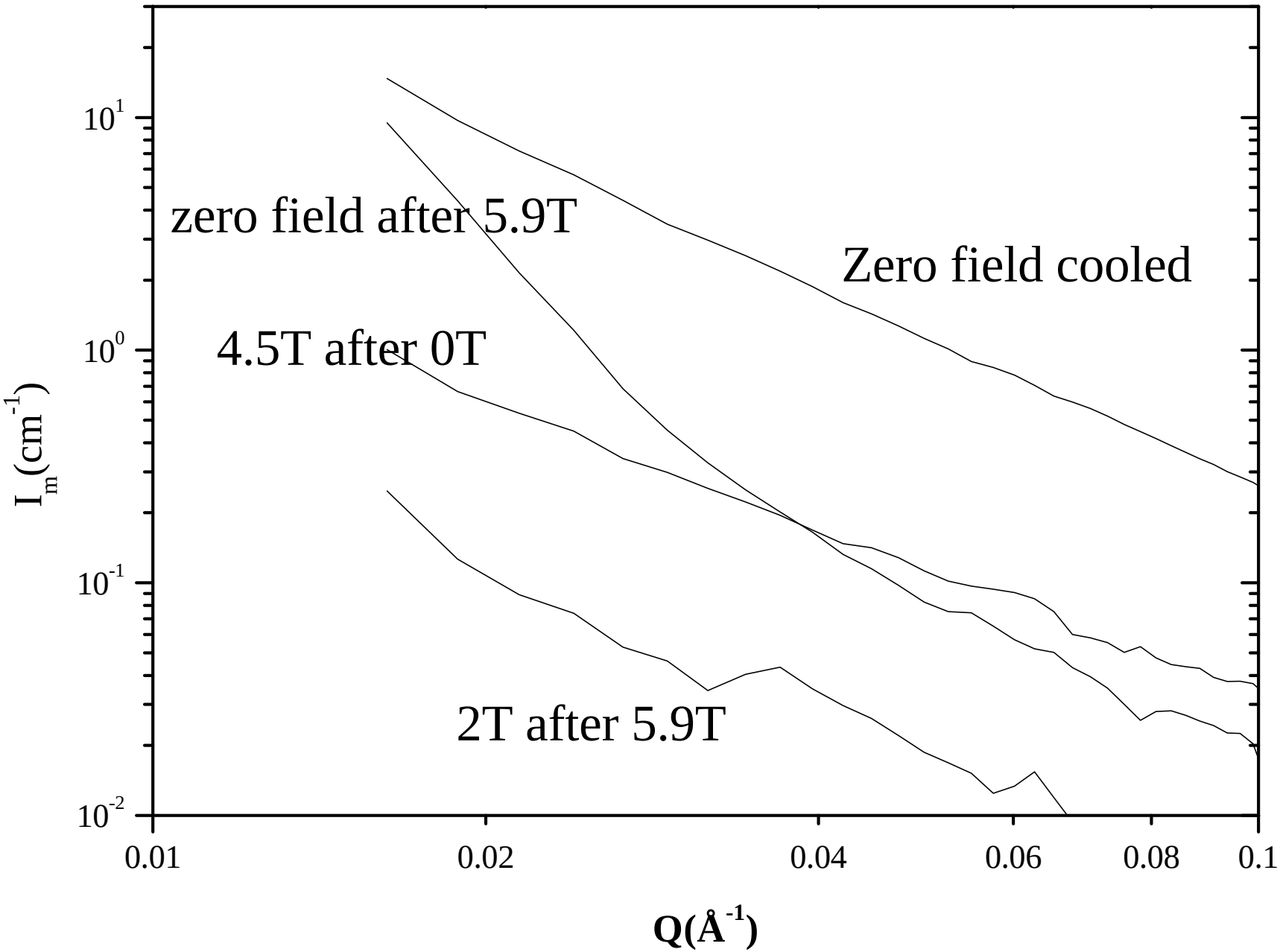
[13] J.A. Fernandez-Baca et al., Phys. Rev. B66, 054434 (2002).

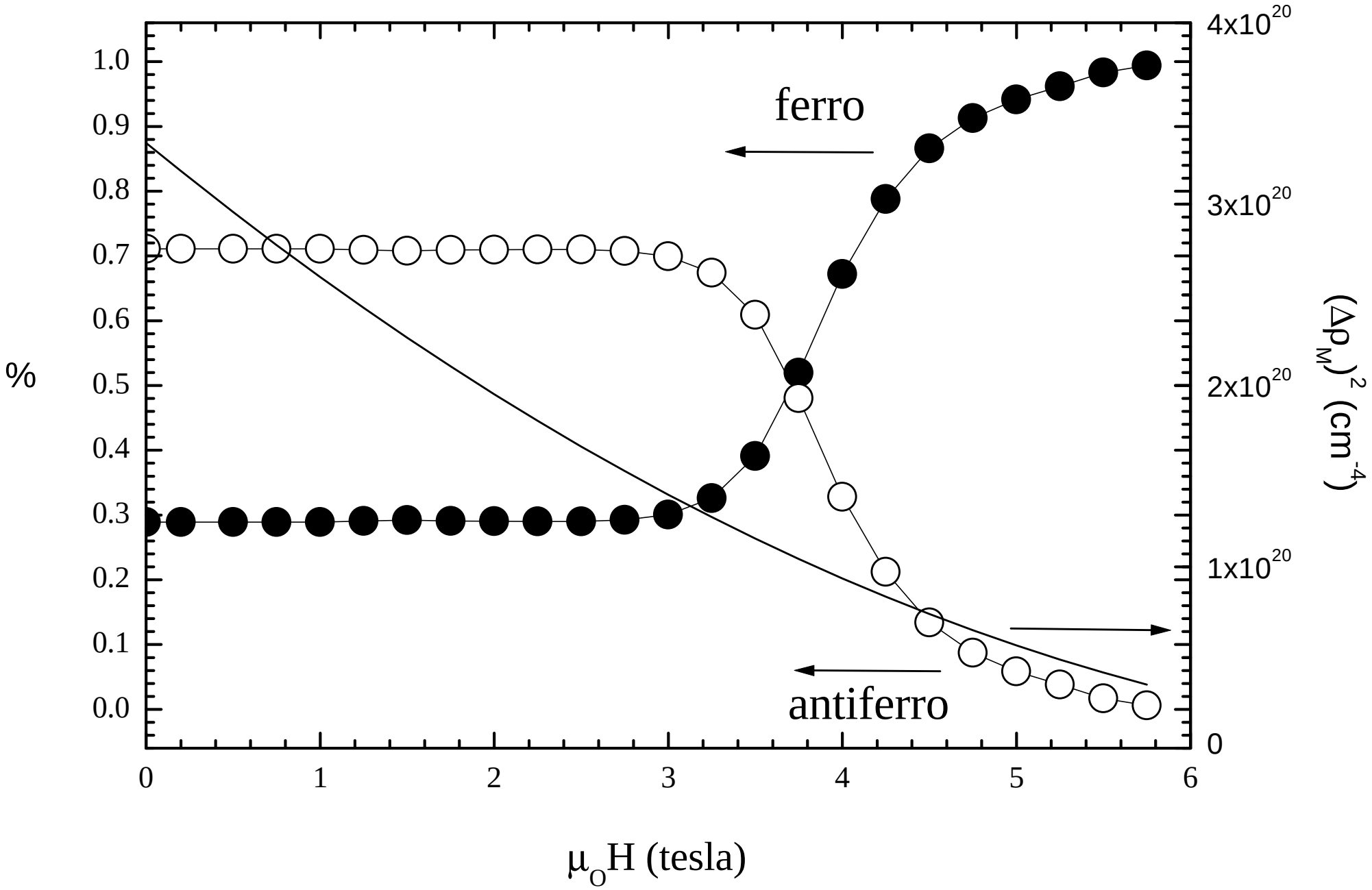

M ($\mu_B$/f.u.)
$\mu_o$H (T)
0T down
0T up
2T up
4T up
6T
$\mu_o$H

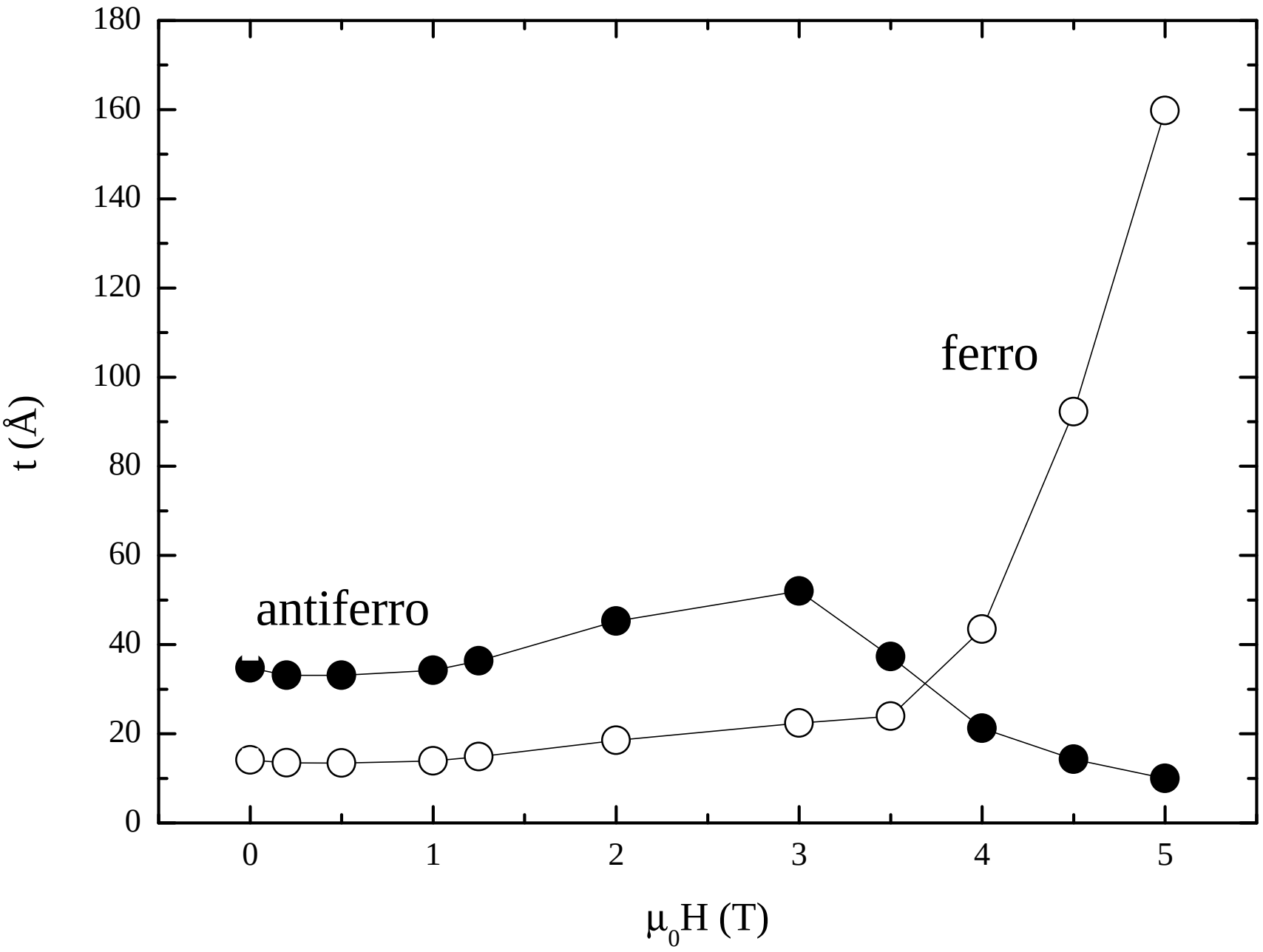

(a)
(b)
0,2
0,1
0,0
-0,1
-0,2
Q_y (Å^-1)
-0,2
-0,1
0,0
0,1
0,2
Q_x (Å^-1)


0T
2T
4T
4.5T
5T
$10^{1}$
$10^{0}$
$10^{-1}$
$10^{-2}$
$I_m(cm^{-1})$
0.01
0.02
0.04
0.06
0.08
0.1
Q(Å$^{-1}$)


10000
1000
100
10
1
0.1
0.01
0.01
0.1
$I_m$ ($cm^{-1}$)
Q($A^{-1}$)
B=0
B=4T
30K
$Q^{-4}$
$Q^{-2}$


zero field after 5.9T
Zero field cooled
4.5T after 0T
2T after 5.9T
$10^{1}$
$10^{0}$
$10^{-1}$
$10^{-2}$
$I_m$ ($cm^{-1}$)
0.01
0.02
0.04
0.06
0.08
0.1
Q(Å$^{-1}$)


ferro
antiferro
%
1.0
0.9
0.8
0.7
0.6
0.5
0.4
0.3
0.2
0.1
0.0
0
1
2
3
4
5
6
μ_O H (tesla)
4x10^20
3x10^20
2x10^20
1x10^20
0
(Δp_M)^2 (cm^-4)


180
160
140
120
100
80
60
40
20
0
t (Å)
0
1
2
3
4
5
μ0H (T)
antiferro
ferro